Aerodynamics in the classroom and at the ball park

Rod Cross*

Department of Physics, University of Sydney, Sydney NSW 2006, Australia

Abstract

If the gravitational force on a projectile is larger than the aerodynamic forces then the trajectory is usually close to parabolic. In the opposite limit, the trajectory can be quite different. A light ball with sufficient backspin can curve vertically upward through the air, defying gravity and providing a dramatic visual demonstration of the Magnus effect for classroom demonstration purposes. A ball projected with backspin can also curve downward with a vertical acceleration greater than that due to gravity if the Magnus force is negative. These effects were investigated by filming a light polystyrene ball and a large diameter ball projected in an approximately horizontal direction so that the lift and drag forces could be easily measured. The balls were also fitted with artificial raised seams and projected towards a vertical target in order to measure the sideways deflection over a known horizontal distance. It was found that (a) a ball with a seam on one side can deflect either left or right depending on its launch speed and (b) a ball with a baseball seam can also deflect sideways, depending on the orientation of the seam, even when there is no sideways component of the drag or lift forces acting on the ball.

I. INTRODUCTION

The flight of a spherical ball through the air and the effects of aerodynamic drag and lift have been described in many articles in this journal[1–5] and elsewhere.[6–8] The drag force acts in a direction opposite the velocity vector and acts to reduce the ball speed. A lift force on a spherical ball arises when the ball is spinning and is known as the Magnus force.[1,4,6] The Magnus force acts in a direction perpendicular to both the velocity vector and the spin axis. An additional sideways force can act on a ball if it has a raised seam or if one side of the ball is rougher than the other. If the orientation of the seam and/or the rough and smooth sides of the ball is asymmetrical in a direction transverse to the flight path then there is an asymmetry in the flow of air around the ball, resulting in a sideways force on the ball.

Aerodynamic forces and the corresponding drag and lift coefficients are most commonly measured in wind tunnel experiments. It is relatively easy to calculate the trajectory of a ball if the relevant forces on the ball are known. The inverse problem is generally more difficult. That is, it is usually a difficult task to calculate the aerodynamic forces in terms of measured trajectories. Part of the problem is that the dominant force on a ball in flight is usually the gravitational force, in which case aerodynamic forces result in only a small perturbation to the parabolic trajectory. An additional problem is that large errors can result when the ball coordinates are differentiated to calculate the velocity and then differentiated again to calculate the acceleration of the ball. If the acceleration of the ball is only slightly different from the acceleration due to gravity, then the inferred aerodynamic forces can be subject to large measurement errors.

In this paper, experimental data are presented on the trajectories of light balls, the primary objective being to provide insights into the origin and magnitude of the aerodynamic forces acting on the balls. A second objective was to show that the aerodynamics of lift, drag and side forces can all be illustrated in a dramatic manner, suitable for classroom demonstration purposes, using light polystyrene balls. A light ball that is spinning curves more rapidly and over a shorter distance than a heavy ball, and can effectively defy gravity by rising rather than falling through the air. Alternatively, if the ball is projected in a horizontal direction and if the vertical lift force is equal to the gravitational force, then the ball can follow a "zero gravity" straight line path through the air rather than the more familiar parabolic trajectory. An advantage of using light balls in this context, in addition

to the safety aspect, is that aerodynamic forces on a ball can be measured more accurately when the gravitational force is relatively weak.

Many experiments have previously been described on measurements of g and the drag force on a ball falling vertically through the air or through a liquid.[9–11] Only a few experiments have been reported where aerodynamic forces were derived from measured ball trajectories[12–14] or from a ball passing through light gates.[15] Effects of ball seams and roughened surfaces have previously been studied for specific sports ball types including baseballs[2,4,7,15], cricket balls[15–18] and soccer balls[19]. The raised stitching of a baseball is known to affect the flight path of a slowly spinning knuckleball, although the stitching has not previously been found to affect the flight of other pitched baseballs. In this paper evidence is provided that the stitching can also affect the flight of a rapidly spinning baseball.

Asymmetric air flow around a cricket ball has been studied primarily in relation to a phenomenon known as reverse swing.[7,16–18] Under some conditions, a cricket ball can curve sideways in the "wrong" direction. When a cricket ball is new, both sides of the ball are smooth and the asymmetry in air flow is due to alignment of the stitching. Unlike a baseball, the stitching of a cricket ball runs around the equator, and it is usually aligned by the bowler at an angle of about 20° to the path of the ball. With a new ball, reverse swing occurs only at ball speeds above about 90 mph. A cricket ball develops a rough and a smooth side during match play, in which case reverse swing can occur at lower speeds since surface roughness adds to the effect of the raised seam in generating turbulent air flow around the ball. Players deliberately polish one side of the ball during a match in order to maintain the asymmetry. If one side of the ball is rough enough then reverse swing can be achieved even when the stitching is aligned parallel to the air flow, in which case the asymmetry in the air flow is due entirely to the fact that one side of the ball is rougher than the other.

A disadvantage in studying real sports balls is that the geometry can be complicated by the curved shape of the stitching or by the fact that the stitching needs to be aligned at an angle to the flight path. The latter problem is not an issue when examining air flow in a wind tunnel since the ball can simply be rotated at any desired angle to the air flow. In the present experiment the effects of ball asymmetry were studied in a simpler manner, more suited as an undergraduate project, by projecting a ball with backspin to measure the deviation in its path caused both by the Magnus force and by a left–right asymmetry. The balls were projected with backspin to stabilize the orientation of the ball and to allow the

left or right sideways force to be measured independently of the gravitational and Magnus forces acting in the vertical plane.

II. ORIGIN OF SIDEWAYS FORCES

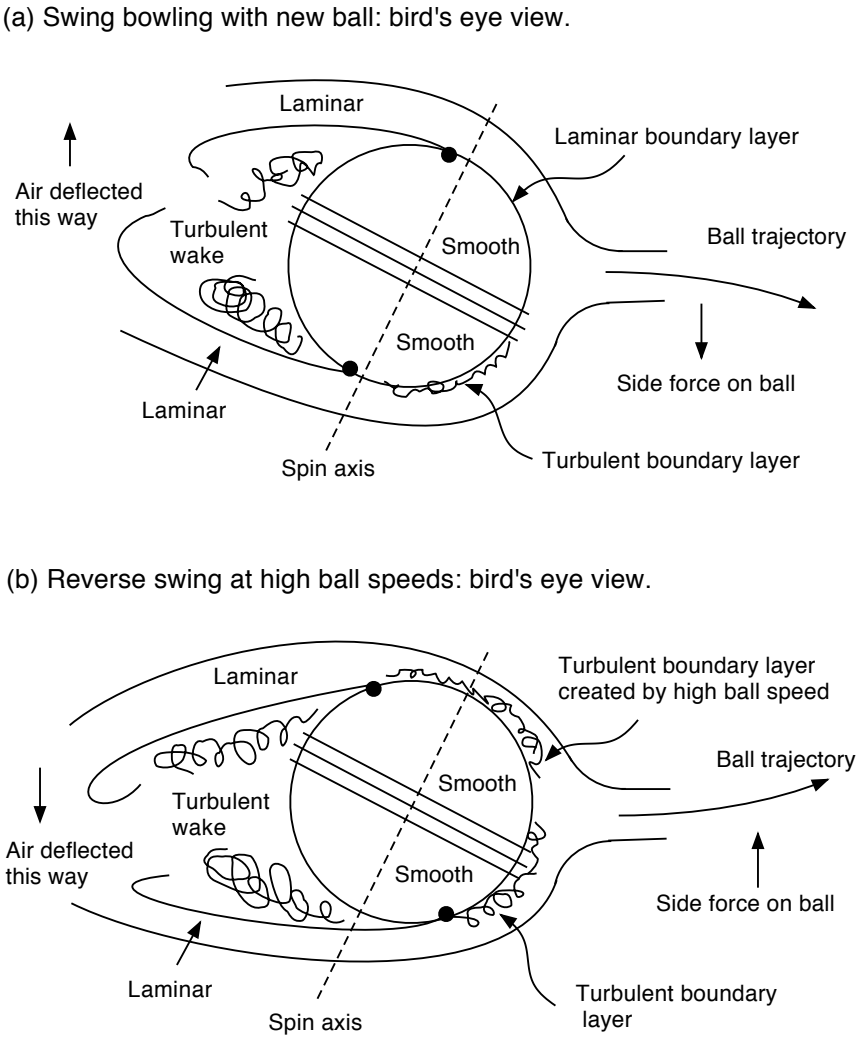

FIG. 1: (a) Conventional swing of a new cricket ball results from the asymmetric air flow around the ball. The stitching is inclined at about 20° to the ball path and is maintained in that orientation by rotation of the ball about an axis perpendicular to the stitching. Black dots denote the separation points. (b) Reverse swing of a new ball occurs at high ball speeds due to asymmetrical separation of the turbulent boundary layers on each side of the ball.

It is well known that the flow of air around an object in flight can be asymmetrical in both the front–to–back and transverse directions, especially if the object itself is asymmetrical. The front–to–back asymmetry contributes to the drag force, the air pressure at the front of a projectile being larger than the pressure at the rear. In the case of a sphere, asymmetrical air flow in the transverse direction can be induced either by spinning the ball, in which case the asymmetry results in a Magnus force, or by modifying the surface of the sphere so that the sphere is asymmetrical in a transverse direction. For example, one side of a sphere might be rougher than the other. An asymmetry of the latter type results in a side force that can arise even if the sphere is not spinning. Regardless of the source of the asymmetry, if the air is deflected downwards by a ball in flight then the air exerts an equal and opposite force upwards on the ball. Similarly, if the air is deflected to the left by the ball, then the air exerts an equal and opposite force to the right on the ball. Deflection of the air flow is caused by early separation on one side of the ball and late separation on the other side. To illustrate how a side force can arise in practice, we will consider the case of a new cricket ball with a raised seam, as shown in Fig. 1.

Separation is a boundary layer effect whereby air flowing in a thin layer adjacent to the ball surface is slowed by friction until it comes to rest at the separation point. Air remains at rest right at the surface itself, increasing in speed away from the surface in the thin boundary layer, while the air speed in the boundary layer decreases in a direction along the surface. At the separation point, $\partial v/\partial y = 0$ where v is the air speed along the surface and y is the coordinate perpendicular to the surface. Air is deflected away from the surface at the separation point, in a direction approximately tangential to the surface. Consequently, the net transverse flow of air in Fig. 1(a) is upward in the figure (actually to the left side of the ball, Fig. 1 being a bird's–eye view) since air separates later on the right side of the ball than the left side.

Typically, the separation point on a sphere is near the equator on both sides of the ball, at least if the ball surface is smooth and the air flow remains laminar in the boundary layer. If one side of the ball is rough or if it has a raised seam, then the air flow in the boundary layer will become turbulent and separate from the ball further towards the rear of the ball. Turbulent air in the boundary layer mixes with higher speed air at the outer edge of the boundary layer, thereby increasing the average air speed near the ball surface and delaying separation. However, if turbulent air encounters a raised seam, then the boundary layer is

thickened[18] and the separation point remains near the equator, as indicated in Fig. 1(b). At high ball speeds, air in the boundary layer can become turbulent even if the ball surface is smooth. In that case, air flows in turbulent boundary layers on both sides of the ball regardless of whether one side is rough or contains a raised seam. Delayed separation on both sides of the ball acts to reduce the drag coefficient, resulting in a so–called drag crisis.[3] As the ball speed increases the side force can therefore decrease to zero and may then reverse sign with a further increase in ball speed. The latter effect is responsible for reverse swing in cricket and occurs at Reynolds numbers above about 2×10^5 for a new ball or at ball speeds above about 90 mph.

III. EXPERIMENTAL DETAILS

Aerodynamic forces acting on a ball in flight increase with the speed and diameter of the ball but do not depend on the mass of the ball. The trajectory of a light ball therefore provides a more sensitive measure of the effect of the aerodynamic forces. An additional advantage of a light ball is that large changes in ball speed and direction occur over a short path distance and can be observed with a single or with two cameras rather than needing many such cameras to record the trajectory over a long flight path.[13] A disadvantage is that a light ball is also more sensitive to the effect of wind. Experimental data was collected outdoors only when the air was still. On windy days, the experiment was conducted in a lecture theatre using overhead projectors to illuminate the ball. The trajectory of each ball was filmed at high frame rates using relatively inexpensive cameras. One camera (a Casio EX-F1) was used to film at 300 frames/s, and a second camera (a Canon SX220HS) was used to film at 120 frames/s viewing at right angles to the first camera.

Table 1. Mass (M) and diameter (D) of the balls used in the experiments

No.	Ball	M (g)	D (mm)
1	Polystyrene A	8.98	101
2	Polystyrene S	12.15	98
3	Polystyrene BB	11.55	100
4	Hollow Plastic	92	228

Properties of the balls selected for this study are shown in Table 1. The three polystyrene balls were nominally the same but one (S) was fitted with a circular loop of string glued to the ball to simulate a straight seam and one (BB) was fitted with an artificial baseball seam made from string and glued to the ball, as indicated in Fig. 2. In both cases, the string diameter was 1.5 mm. For ball 2, the string was offset from the center by a distance $b = 30$ mm. The baseball seam was scaled directly from measurements of the stitching on an actual baseball. Polystyrene ball A was unmodified. The hollow plastic ball was smooth, apart from a small indentation used to inflate the ball. It was manufactured as a child's basketball and was slightly larger in diameter than an approved soccer ball (218 - 221 mm).

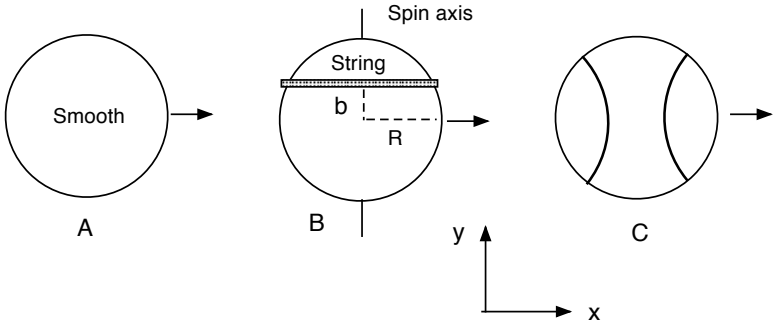

FIG. 2: The three types of ball used in this study. (a) smooth ball, (b) smooth ball modified by gluing a circular loop of string around the ball to simulate a raised seam, and (c) smooth ball modified by gluing a single length of string to the ball as an artificial baseball seam. Each ball was projected in the x direction with backspin.

An attempt was made to launch hollow rubber balls at high speed using a tennis ball launcher but the raised seam glued to the ball resulted in an asymmetrical launch with unwanted sidespin. Consequently, rubber balls were not used. The balls listed in Table 1 were launched either by hand at relatively low speed and low spin or at higher speed and spin with a home–made lacrosse type ball launcher. The launcher was constructed from a 1.5 m length of 5 mm diameter aluminum rod, bent into the shape shown in Fig. 3, and bolted to a rectangular wood handle. When launching the type B ball shown in Fig. 2, the string seam did not come into contact with the launcher so sidespin could be avoided. The lacrosse launcher was swung either by hand or by pivoting it in a frame using an elastic bungee cord to swing it more precisely at controlled and adjustable speeds. No attempt was made to control the ball speed and spin separately, with the result that the spin imparted to

the ball was approximately proportional to the launch speed, both when throwing by hand and when using the lacrosse launcher.

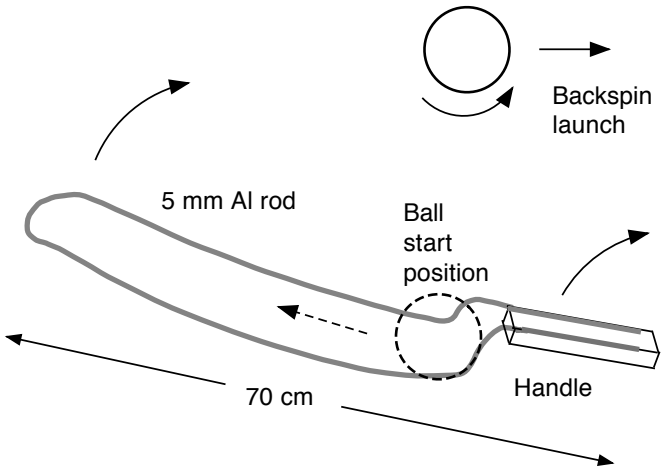

FIG. 3: Lacrosse type launcher used to throw balls.

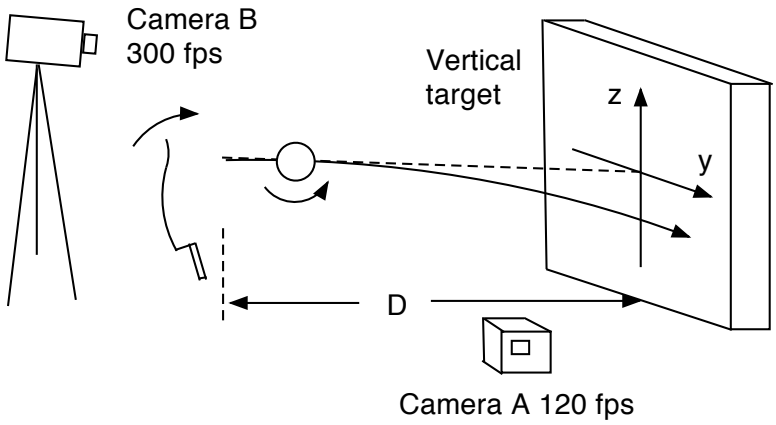

FIG. 4: Experimental arrangement used to measure the vertical (z) and horizontal (y) deviation of a ball over the horizontal distance D from the launch point to the impact point with a vertical target. Camera A was used to record the ball trajectory in the vertical $x-z$ plane, while camera B was used to measure the horizontal launch angle, the ball spin and the impact point on the target.

Three separate experiments were undertaken using balls selected from Table 1. In Experiment 1, balls 1 and 4 were projected in an approximately horizontal direction with backspin to measure the lift and drag forces. Ball 1 was projected outdoors at speeds up to 28 ms^{-1} and was observed to climb vertically to a height of about 4 m before falling back to the

ground. In that experiment, the vertical acceleration of the ball was about 65 ms^{-2} and the horizontal acceleration was about -90 ms^{-2} at the beginning of the launch, the acceleration in both directions being much larger than the gravitational acceleration. Under some conditions (described in Sections V and VIII) the vertical acceleration of Ball 4 was found to be about -17 ms^{-2}, indicating that the Magnus force can sometimes be negative.

Experiment 2 was conducted by projecting ball 2 in an approximately horizontal direction to impact a vertical target located 5 m from the launch point, as shown in Fig. 4. The target consisted of four 80 cm square rubber mats attached to a vertical wall, each marked with a 10 cm grid so the impact point could be measured accurately from video film. The ball was launched nominally at right angles to the target but small errors in the vertical and horizontal launch angles were monitored by the two cameras so that the vertical and horizontal deviations of the ball could be measured more accurately. The impact point on the target could be measured to within 1 cm, but the horizontal deflection of the ball over the 5 m distance to the target could be measured to an accuracy of only about 9 cm, corresponding to an error of about one degree in the measured accuracy of the horizontal launch angle. In other words, if the ball was launched one degree away from the normal then zero deflection would correspond to an impact on the target displaced 9 cm horizontally from the impact point for a ball launched exactly normal to the target.

The horizontal deflection of each ball also depends on the orientation of the spin axis and on the orientation of the seam with respect to the spin axis. If the spin is not pure backspin then the ball can be projected sideways as a result of a sideways component of the Magnus force. If the seam is tilted with respect to the spin axis then the orientation of the seam with respect to the launch direction varies during each revolution of the ball. Both of these effects were present to some extent in most cases, but the effects were minimised by selecting for analysis only those balls launched with almost pure backspin and with the seam properly aligned.

Experiment 3 was performed in essentially the same manner as Experiment 2, using the polystyrene ball with a baseball seam. The ball was launched by hand with backspin, varying the orientation of the seam on a trial and error basis in order to maximize the sideways deflection. Experiment 3 was performed when Professor Alan Nathan sent the author a video clip showing a baseball deflecting sideways in the opposite direction to the direction expected from the Magnus force. The effect was first noticed by Mike Fast, an enthusiast who

contributes regularly to internet articles on the technical aspects of baseball. A video clip of the reverse swinging baseball can be viewed at http://go.illinois.edu/physicsofbaseball. Video film of the experiments described in this paper can be seen on the author's home page at www.physics.usyd.edu.au/∼cross.

IV. DATA ANALYSIS

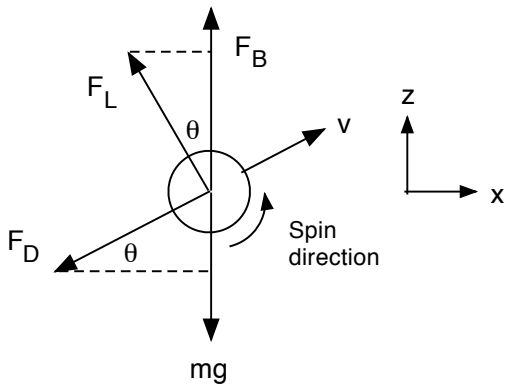

FIG. 5: The forces acting in the $x-z$ plane on a ball with backspin include the gravitational force, mg, the drag force, F_D, the lift or Magnus force, F_L and the buoyant force, F_B.

Consider a ball of mass m that is traveling in the vertical $x-z$ plane with backspin at speed v and at an angle θ to the horizontal, as shown in Fig. 5. The main forces on the ball consist of the gravitational force, mg, a drag force F_D acting in a direction opposite the velocity vector, and a lift force F_L acting in a direction perpendicular to the velocity vector. For relatively light or large balls, the vertical buoyant force, $F_B = m_A g$ may also be significant, where m_A is the mass of air displaced by the ball. A subtle point is that m cannot be measured directly on a scale since the scale reading is $m - m_A$. For each ball tested, m was therefore determined by adding m_A to the scale reading. The equations of motion describing the trajectory are

$$ma_x = -F_D \cos\theta - F_L \sin\theta \tag{1}$$

and

$$ma_z = F_L \cos\theta - F_D \sin\theta - mg + m_A g \tag{2}$$

where a_x is the horizontal acceleration and a_z is the vertical acceleration. From Eqs. (1)

and (2) we find that

$$F_D = -[(m - m_A)g\sin\theta + m(a_x\cos\theta + a_z\sin\theta)] \tag{3}$$

and

$$F_L = (m - m_A)g\cos\theta + m(a_z\cos\theta - a_x\sin\theta) \tag{4}$$

By filming the trajectory of a ball it is possible to estimate a_x, a_z and θ at all points along the trajectory and to calculate the drag and lift forces at each point. The main difficulty with this approach is that small digitizing errors in the measured coordinates $x(t)$ and $z(t)$ can lead to large errors in the acceleration components a_x and a_z, especially if the raw data is differentiated directly. The measured coordinates were therefore fitted with low order polynomials to smooth out small errors, including those due to pixel resolution of the cameras. In those cases where the ball speed decreased by less than about 20% over the measured path length, satisfactory results were obtained by fitting quadratic curves to the measured coordinates, in which case average values of the lift and drag coefficients could be obtained over the measured path. However, if the ball speed decreased by more than about 20% then constant values of the acceleration components could not be assumed and better results were obtained by fitting cubic or higher order polynomial curves to the position coordinates. In the latter case, the acceleration of the ball varied with time, allowing for a measurement of the variation in the drag and lift coefficients with velocity during a single ball throw.

Particular care was taken to ensure that an appropriate polynomial was chosen to fit the data without introducing significant additional errors. The fitted curves were differentiated to obtain the velocity components v_x and v_z and differentiated again to obtain a_x and a_z. The angle θ was obtained from the slope v_z/v_x, and g was taken as 9.81 ms^{-2}. It is emphasized that this approach is feasible only when using relatively light balls. In almost all cases where trajectory data has previously been used to determine drag and/or lift coefficients, including references 12–14, the procedure adopted has been to fit the trajectory data with numerically computed trajectories. In the latter approach, the lift and drag coefficients can be chosen to minimise differences between the data and the computational fit.[14] The approach outlined here does not require any assumptions regarding the variation of the lift and drag coefficients with ball speed or spin. A numerical trajectory cannot be computed without such an assumption.

Conventionally, drag and lift forces are expressed in the form

$$F_D = 0.5 C_D \rho A v^2 \qquad \text{and} \qquad F_L = 0.5 C_L \rho A v^2 \tag{5}$$

where ρ is the density of air, A is the cross–sectional area of the projectile, v is the ball speed, C_D is the drag coefficient and C_L is the lift coefficient. The side force, F_S, arising from a ball seam or from surface roughness can be expressed in a similar manner as $F_S = 0.5 C_S \rho A v^2$, where C_S is the side force coefficient.

At low speeds or at low Reynolds numbers, C_D is about 0.5 for a sphere. Reynolds number is given by $\mathrm{Re} = dv\rho/\eta$ where d is the ball diameter and η is the viscosity of air. Since $\eta = 1.81 \times 10^{-5}$ Poise and $\rho = 1.21$ kg.m^{-3} at room temperature, $\mathrm{Re} = (6.7 \times 10^4 \text{ s.m}^{-2})\, dv$. Wind tunnel measurements show that C_D decreases sharply at $\mathrm{Re} \sim 3 \times 10^5$ for a smooth sphere due to the onset of turbulence in the boundary layer.[3,7] The critical value of Re at which turbulence occurs is reduced by a factor of about two or three if the surface of the sphere is rough or if the boundary layer is tripped into turbulence by a raised seam. For the 100 mm diameter balls used in this study, $\mathrm{Re} = 1 \times 10^5$ at $v = 15$ ms^{-1}. For the 228 mm diameter ball, $\mathrm{Re} = 1 \times 10^5$ at $v = 6.6$ ms^{-1}.

V. EXPERIMENT 1: DRAG AND LIFT FORCE RESULTS

Ball 1 was projected over a wide range of speeds, either by hand or with the aid of the lacrosse launcher. The most interesting results were obtained when swinging the lacrosse launcher by hand to launch the ball at high speed and with backspin at around 2000 rpm. In that case, and if the ball was projected at an angle slightly below the horizontal, the ball straightened out to travel approximately parallel to the ground for a few metres and then climbed steeply upwards by a few metres before falling back to the ground. A typical result is shown in Fig. 6(a). A similar effect was obtained by swinging the launcher in an approximately horizontal plane rather than in the vertical plane, in which case the Magnus force caused the ball to curve rapidly in the horizontal plane. A small backspin component was sufficient to prevent the ball falling out of the horizontal plane while the sidespin component caused the ball to curve rapidly to the right (the author being right–handed). These effects can be shown in a classroom, without danger of injuring students, since polystyrene balls are typically only ten grams or less, are soft, and can be projected toward the ceiling

or away from the class if thought necessary.

The $x(t)$ and $z(t)$ results from Fig. 6(a) were fitted with sixth order polynomials to calculate the v_x and v_z velocity components and differentiated again to obtain the acceleration components. The lift and drag forces were then calculated using Eqs. (3) and (4) in order to calculate the drag and lift coefficients. The results are shown in Fig. 6(b) and in Fig. 7, all obtained from the single throw shown in Fig. 6(a). Multiple throws were not used or needed to construct these results. Figure 7(b) shows a more conventional plot of the lift coefficient vs the spin parameter $S = R\omega/v$ where $R\omega$ is the peripheral speed of the ball. For most ball types, C_L increases from zero to about 0.3 as S from zero to about 0.4 and then remains approximately constant at about 0.3 when S is greater than 0.4.[13,14] For the polystyrene ball, C_L continued to increase up to about $S = 1$. Rapid deceleration of the ball may have affected the aerodynamics in a way that is not commonly observed with heavier balls.

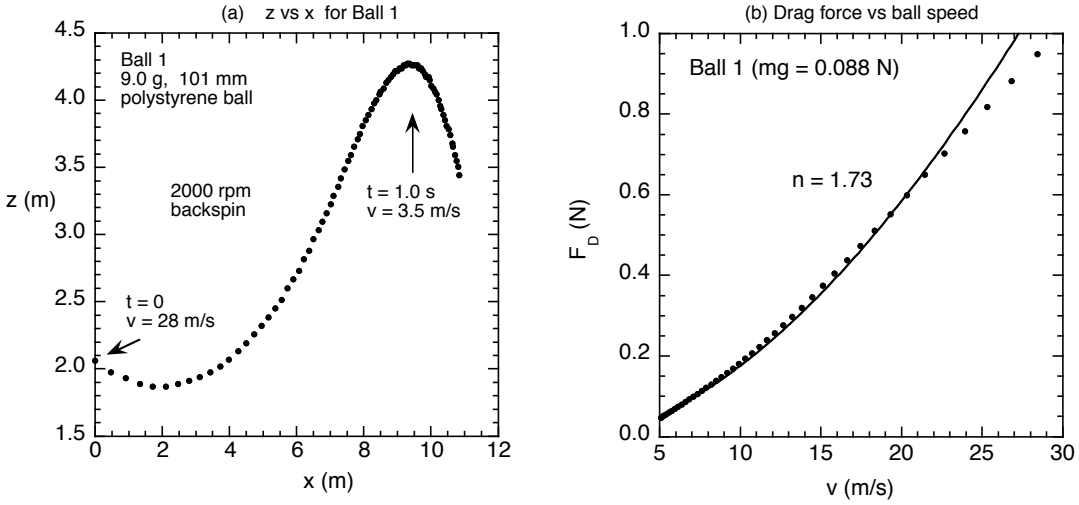

FIG. 6: Results obtained with a 101 mm diameter polystyrene ball launched with backspin at 28 ms^{-1} showing (a) z vs x and (b) the drag force, F_D, vs ball speed, v. Experimental data points are shown at intervals of 1/60 s. The curved line in (b) is a best fit power law of the form $F_D = kv^n$, giving $n = 1.73$.

The drag force was not proportional to v^2 since C_D did not remain constant as the ball speed varied. A best fit power law of the form $F_D = kv^n$ is shown in Fig. 6(b), indicating that $n = 1.73$. As shown in Fig. 7(a), C_D increased from an initial value of about 0.24 to about 0.4 as v decreased. At ball speeds less than about 5 ms^{-1} the drag and lift forces on the ball dropped below the gravitational force and the curve fitting technique used to

calculate the acceleration of the ball was not sufficiently accurate to obtain reliable estimates of the drag and lift coefficients. The low speed drag coefficient of the ball was measured in a separate experiment as 0.5 ± 0.2 by dropping the ball vertically from rest and filming the fall over a drop height of 3 m. As indicated by the large error in C_D, this technique was not very successful since the ball speed could be measured to only about $\pm 2\%$ with the video technique. At $C_D = 0.5$, the theoretical increase in ball speed was 0.48 ms^{-1} over the last 1 m of the fall, whereas the measured increase was 0.48 ± 0.2 ms^{-1}. A better result was obtained using a crude wind tunnel consisting of a fan at one end of a 45 cm long conical tube with an 18 cm diameter exit. The tube was constructed from a rolled–up sheet of plastic. An anemometer was used to measure the wind speed 10 cm beyond the exit and the ball was then placed at the same location, suspended as a 1.1 m long pendulum by two lengths of cotton thread forming a V–shape support to minimise sideways deflection. The thread was attached to the ball with 0.1 g of adhesive tape. The angular displacement of the pendulum was used to calculate the drag force, giving $C_D = 0.55 \pm 0.05$ over the range $2.8 < v < 4.2$ ms^{-1}.

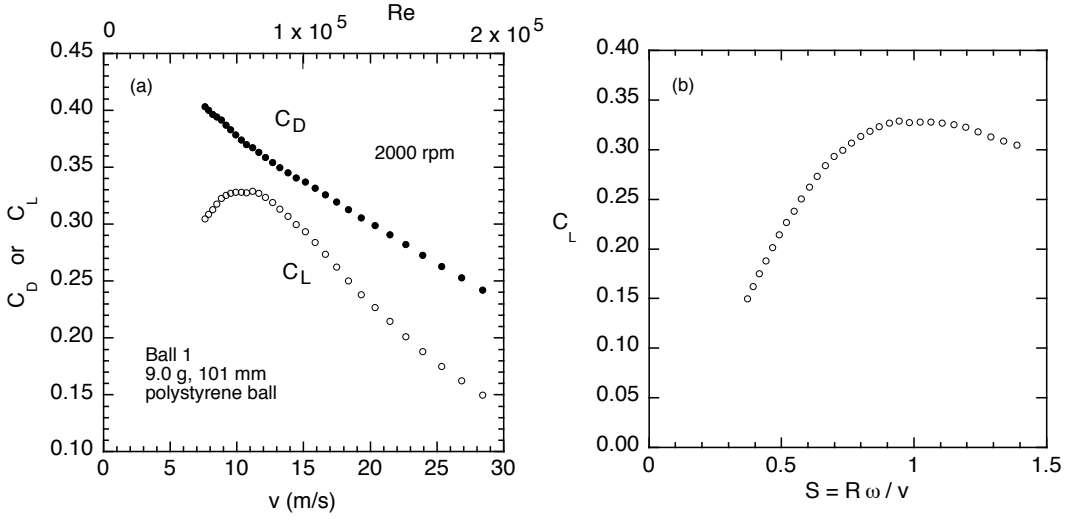

FIG. 7: (a) Drag and lift coefficients calculated from the data shown in Fig. 6, with Reynolds number, Re, on the top axis. (b) The lift coefficient as a function of the spin parameter $S = R\omega/v$ where R is the ball radius.

Results obtained with Ball 4 are shown in Figs. 8 and 9. Low speed results from hand throws were obtained with $\omega \sim 100-200$ rpm, while higher speed results were obtained using the lacrosse launcher with $\omega \sim 350-600$ rpm. Ball 4 was about ten times heavier than Ball

1 so its horizontal velocity decreased by a relatively small amount over a horizontal distance of 3 m, as a result of the drag force, compared with Ball 1. The drag and lift forces were therefore measured as a function of ball speed by throwing the ball many times at different initial speeds. For each throw, time average values of v, C_D and C_L were calculated over the first 2 m of the path length and then plotted as a function of v, as shown in Fig. 9. Scatter in the data for C_L can be attributed in part to the variation in ball spin from one throw to the next. Results from one of the throws are shown in Fig. 8. The x and z coordinates were fitted with low order polynomials and the results indicated that the lift force was negative at ball speeds in the range $9 < v < 14$ ms^{-1} even though all balls were thrown with backspin. For example, in Fig. 8(a), z decreased from a maximum value of 1.88 m at $t = 0.085$ s to $z = 1.59$ m at $t = 0.3$ s. From the relation $\Delta z = 0.5 a_z (\Delta t)^2$ we find that the average acceleration in the negative vertical direction during that time was $a_z = 12.5$ ms^{-2}, larger than g despite the fact that the drag force had a component acting vertically upward during that time.

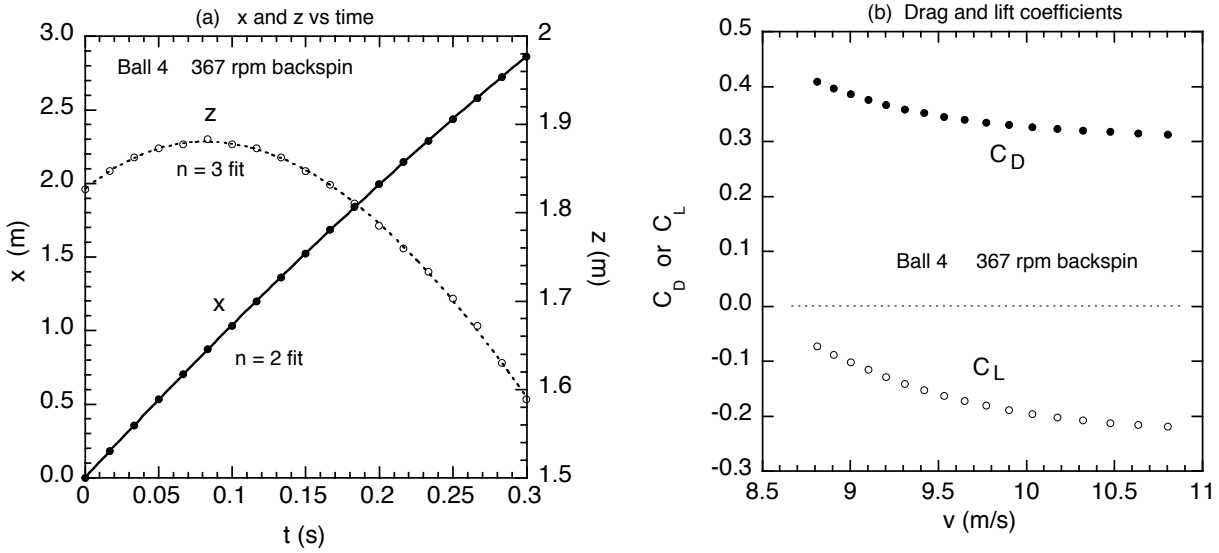

FIG. 8: Results obtained with a 228 mm inflatable plastic ball launched with backspin at 10.8 ms^{-1} showing (a) x (left scale) and z (right scale) vs time and (b) values of the drag coefficient, C_D, and the lift coefficient, C_L, calculated from the results in (a). The solid and dashed curves in (a) are best fit polynomials of order $n = 2$ and $n = 3$ respectively. Experimental data points are shown at intervals of 1/60 s.

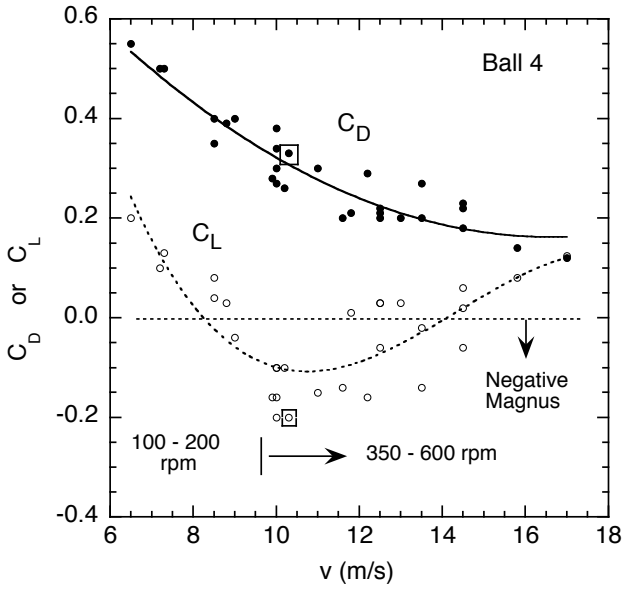

FIG. 9: Drag and lift coefficients for the 228 mm plastic ball vs ball speed, v. Each data point corresponds to a different throw. Results for the two boxed data points are shown in Fig. 8. The solid and dashed lines are best fit curves to the experimental data.

VI. EXPERIMENT 2: SIDE FORCE RESULTS

Results obtained with Ball 2 are shown in Fig. 10. This ball was fitted with an artificial seam of string offset 30 mm from the center of the ball as indicated in Fig. 2B. It was projected with backspin at speeds from 5 ms^{-1} to 17 ms^{-1} in an approximately horizontal direction and with the seam oriented as shown in Fig. 2B. The results in Fig. 10 were obtained with the string on the left of center as viewed by the thrower. When the ball was projected at low speed with the string on the left, the ball deflected to the left, and vice–versa when the string was on the right. The ball also curved in a vertical direction as a result of the Magnus force and the force due to gravity, but the results in Fig. 10 show only the horizontal y deflection (as defined in Fig. 4) or "break" after the ball travelled a horizontal distance of 5 m in the x direction to the vertical target. The ball speed shown in Fig. 10 is the average ball speed over the 5 m distance to the target, as measured from the transit time from the launch point to the target. The ball speed decreased typically by about 45% over this distance.

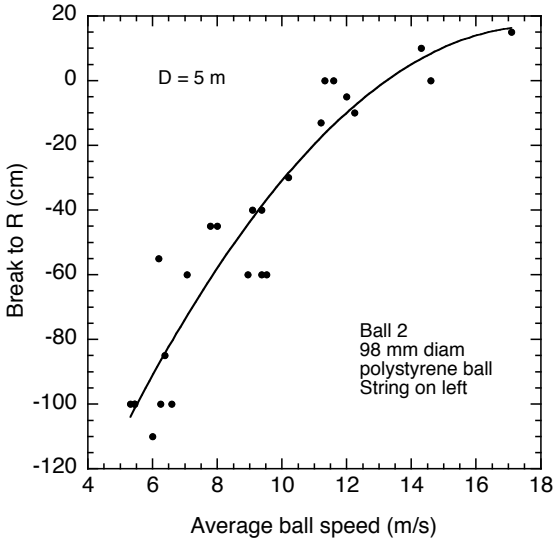

FIG. 10: Sideways break of a 98 mm diameter polystyrene ball plotted as a function of average ball speed over the 5 m distance from the launch point to the target. The ball was fitted with an artificial seam (a circular loop of string) and projected as shown in Fig. 2B with backspin. The curved line is a quadratic fit to the experimental data, each point representing a different throw.

At low ball speeds, the backspin imparted to the ball by hand was about 50 rad.s^{-1} and the ball deflected horizontally by about 100 cm over the 5 m distance to the target. As the launch speed was increased, the amount of backspin also increased and the ball deflected by a smaller amount, reducing to zero at a ball speed about 12 ms^{-1} when the ball spin was about 150 rad.s^{-1}. At higher speeds and spin, the ball deflected in the opposite direction to that observed at low ball speeds.

The side force coefficient, C_S, is typically about 0.2 to 0.3 for a cricket ball with conventional swing. For the polystyrene ball, the largest break was about 100 cm and was observed when the ball was thrown at an initial speed of about 9 ms^{-1}. It traveled the 5 m distance to the target in about 0.8 s at an average speed of about 6 ms^{-1} and with an average sideways acceleration of 3 ms^{-2}. The average side force coefficient for the polystyrene ball was therefore about 0.22 at an average ball speed of about 6 ms^{-1} and it decreased to zero at an average ball speed of about 12 ms^{-1}.

Similar results were obtained with a 150 mm diameter, 23 g polystyrene ball and with a 214 mm diameter, 84 g hollow plastic ball, each fitted with an artificial seam in the manner indicated in Fig. 2B. At ball speeds around 6 to 7 ms^{-1}, the break for each of these balls

was about 80 cm over the 5 m distance to the target, the break decreasing to zero and then reversing direction at ball speeds above about 10 ms^{-1}.

VII. EXPERIMENT 3: EFFECT OF BASEBALL SEAM

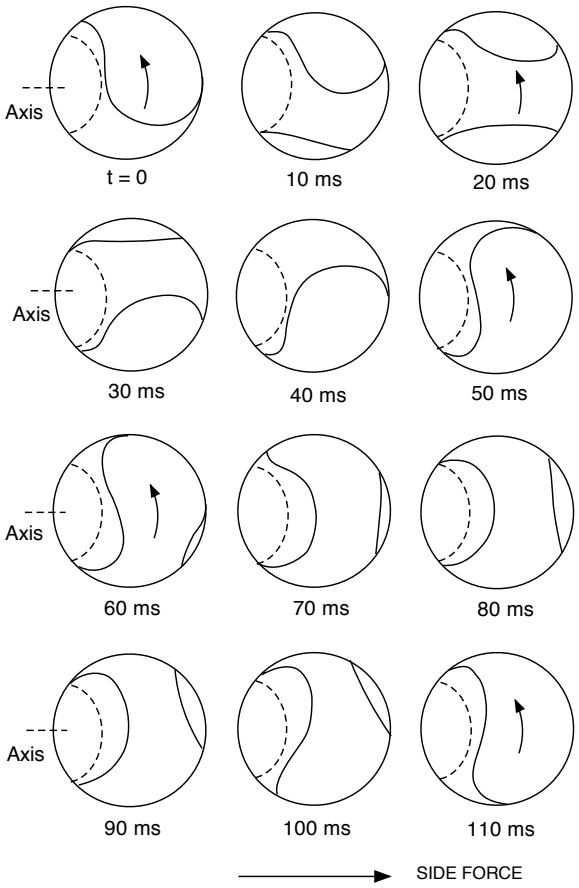

FIG. 11: Rotation of a polystyrene ball with a baseball seam, as viewed by the batter, shown at intervals of 10 ms. The time for one revolution was 126 ms, corresponding to backspin at 474 rpm. The ball was thrown at 11.8 ms^{-1} and curved to the left as viewed by the pitcher or to the right as viewed by the batter. The break in the y direction was 90 cm over a path distance of 5 m in the x direction. The region enclosed by the dashed circle around the axis remained smooth since the seam did not rotate into that region.

The polystyrene ball with a baseball seam, Ball 3, was thrown by hand with backspin at a vertical target located 5 m from the launch point. The launch speed was held at about 10–12 ms^{-1}, corresponding to backspin at about 400–500 rpm, while the orientation of the

seam was varied. The average ball speed over the 5 m distance to the target was about 6 to 7 ms^{-1}. When thrown as a 2–seam or 4–seam fastball (in terms of its orientation rather than speed) the ball did not deflect sideways since the seam remained symmetrical in the y direction. The largest horizontal sideways deflection in the y direction was 90 cm, and was obtained when the ball was oriented as shown in Fig. 11. In that orientation, the spin axis remained horizontal so the Magnus force remained vertical but the spin axis was tilted by about 10° in the x direction.

The ball was filmed at 300 frames/s from behind the thrower, viewing toward the target. Video images were used to reconstruct views of the ball as seen by the batter, shown in Fig. 11 at 10 ms intervals during one full revolution. The result in Fig. 11 was obtained at a launch speed of 11.8 ms^{-1}. The ball took 0.70 s to strike the target so its average speed in the x direction was 7.1 ms^{-1}, and it slowed to about 4.5 ms^{-1} by the time it reached the target. The spin remained constant during the transit to the target.

VIII. DISCUSSION

The three experiments described in this paper have revealed a surprising variety of aerodynamic effects, all of which can be observed in the classroom for demonstration purposes or analyzed simply and safely in an undergraduate laboratory without the need for expensive equipment and without needing a wind tunnel. In the first experiment, the drag and lift forces on a polystyrene ball were measured over a speed range from 7 to 28 ms^{-1} from just one throw of the ball, corresponding to a change in Reynolds number from 47,000 to 1.9×10^5. For a smooth sphere, the drag coefficient remains constant at about 0.5 over this range[3], but if the surface is slightly rough then C_D can drop well below 0.5 even at $\text{Re} = 1 \times 10^5$. The polystyrene ball was not perfectly smooth but consisted of many small segments varying in height by about 0.5 mm. The results for C_D shown in Fig. 7(a) are consistent with this level of surface roughness and consistent with drag force measurements of other balls of similar roughness.[3,7,14,15]

Results obtained with the larger plastic ball, shown in Fig. 9, differ from those obtained with the polystyrene ball in that the lift coefficient was negative at ball speeds from about 9 to 14 ms^{-1}. Such a result is not easily interpreted in terms of Bernouilli's principle, commonly employed in text books to explain the Magnus effect. A reversal in the direction

of the Magnus force has previously been observed in wind tunnel experiments and can be attributed to the fact that the boundary layer can become turbulent on one side of the ball and remain laminar on the opposite side.[1] For example, consider the case shown in Fig. 8 where the ball was spinning at 367 rpm with a peripheral speed $R\omega = 4.4$ ms^{-1}, and translating at $v = 10$ ms^{-1}. The relative speed of the ball and the air was 14.4 ms^{-1} on one side of the ball and 5.6 ms^{-1} on the opposite side of the ball, as indicated in Fig. 12. The local Reynolds number was 2.2×10^5 on the high speed side and 8.5×10^4 on the low speed side. A turbulent boundary layer on the high speed side will separate later than a laminar layer on the low speed side, deflecting air toward the low speed side. The air exerts an equal and opposite force on the ball in a direction from the low speed to the high speed side, in the opposite direction to the conventional Magnus force. At ball speeds less than about 9 ms^{-1} the ball spin was typically about 100 to 200 rpm and the Reynolds number was not high enough for the boundary layer to become turbulent. At ball speeds above about 14 ms^{-1} the boundary layer was presumably turbulent on both sides of the ball, allowing the Magnus force to act in the conventional direction.

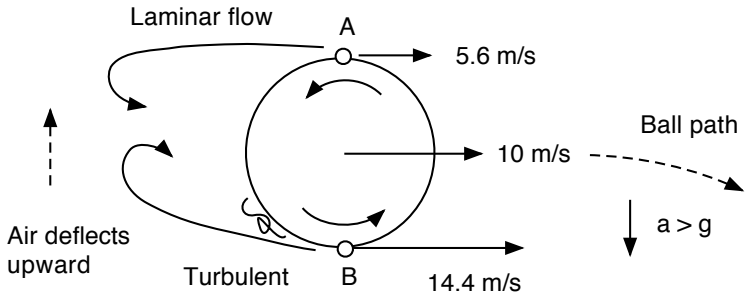

FIG. 12: A negative Magnus force can arise, as shown here for a ball traveling horizontally to the right with backspin, if the air flow is laminar on the upper side of the ball and turbulent on the lower side. In this example, the peripheral speed of the ball due to spin is 4.4 ms^{-1}, the center of mass speed is 10 ms^{-1}, point A translates to the right at 5.6 ms^{-1} and point B translates at 14.4 ms^{-1}. The air flow near A is laminar and the flow near B is turbulent.

The second experiment simulated results that are well known in relation to the behavior of a cricket ball, despite the fact that the ball speed was much lower. Cricket balls are normally projected by fast bowlers at speeds of around 80 to 90 mph and are observed to curve in the "wrong" direction when the ball is new only at speeds of about 90 mph or

more, corresponding to a Reynolds number above about 2×10^5 for a new ball. As shown in Fig. 10, the polystyrene ball was observed to curve sideways in the 'wrong" direction at ball speeds around 15 ms^{-1} (31 mph) or at a Reynolds number about 1×10^5. The differences here are consistent with the facts that the polystyrene ball was slightly rough and was larger in diameter than a cricket ball. The different geometry of the artificial seam may also have contributed to a reduction in the required Reynolds number. On a cricket ball, the seam passes over or under the center of the ball at the top and bottom of the ball (as indicated in Fig. 1) and is offset from the center of the ball by a relatively large distance only near the front or rear of the ball. The seam used on the polystyrene ball was offset from the center of the ball by the same large amount around the whole circumference, as indicated in Fig. 2B.

The results of the experiment with the baseball seam were very surprising since a large sideways deflection due to the seam has not previously been reported. Watts and Ferrer[4] measured the lift force on spinning baseballs in three different orientations and found that the orientation had no effect. They concluded that a spinning baseball behaves as a fully rough sphere regardless of where the seams are located. Watts and Sawyer[2] measured the lateral force on a stationary baseball in a wind tunnel and found that the force does indeed vary with the orientation of the seam and concluded that the lateral force is responsible for the erratic path of a slowly spinning knuckleball. Since those experiments were reported, there has never been any suggestion that the sideways deflection of a rapidly spinning baseball might be due to anything other than the Magnus force. More recent studies of the effects of stitching on baseballs can be found in several theses that are available on the web.[20,21] Alaways[20] found that the side force on a baseball is small since he examined only the symmetrical 2– and 4–seam orientations of the seam. In Experiment 3, the ball was projected with backspin so that the Magnus force acted in a vertical direction, yet a large sideways deflection was observed for some orientations of the seam. The maximum sideways deflection was almost as large as that observed in Experiment 2 using the same type of ball fitted with a simple circular seam.

Inspection of Fig. 11 shows that the seam is essentially vertical and offset to the left side of the ball at 50, 60 and 110 ms and that the vertical part of the seam is offset to the left side at other times as well. Consequently, the time average orientation of the seam is not symmetrical during one revolution of the ball, but is offset to the left of center in a manner similar to that in Experiment 2. In both Experiments 2 and 3, the maximum ball deflection

occurred at the same low ball speeds, but the ball with the baseball seam deflected in the opposite direction to the ball with the offset, circular seam. The ball with the offset seam deflected to the left when the seam was on the left, as viewed by the thrower, or it deflected to the right when the seam was on the right, as viewed by the batter. As shown in Fig. 11, the ball with the baseball seam deflected to the right (viewed by the batter) even though the vertical part of the seam was on the left on average.

The sideways deflection observed in Experiment 3 cannot therefore be due to the same effect as that seen in Experiment 2, nor can it be attributed to the effect responsible for reverse swing of a cricket ball since the largest deflections in Experiment 3 were observed at low ball speeds rather than at high ball speeds. As shown in Fig 11, the ball rotates in such a way that the left side of the ball close to the axis remains smooth at all times since the axis is well removed from the seam in all directions. During part of one revolution, almost the whole of the left side of the ball remains smooth. As the ball rotates, the seam passes through all regions on the right side of the ball and part of the left side of the ball as well. Consequently, a baseball in this orientation can be expected to behave in the same manner as a ball that is uniformly rough on the right side and uniformly smooth on the far left side. The boundary layer will therefore be turbulent on the right side but the behavior of the boundary layer on the left side is less certain.

If the ball was completely smooth on the left side then the boundary layer would remain laminar at low ball speeds. Being partly rough and partly smooth, the boundary layer is likely to be less turbulent on the left side, in which case the separation point on the left side will be closer to the front of the ball than on the right side and air flowing around the ball will be deflected to the left at the rear of the ball. Consequently, the ball will deflect to the right, as observed. In that respect, the effect appears to be very similar to that observed with a scuff ball where one side is illegally roughened. Given that it is possible to generate a large break by roughening a baseball and allowing the spin axis to pass through the rough patch,[22] then the opposite effect is likely to be just as effective. Experiment 3 indicates that a smooth patch around the axis is indeed effective in generating a large break, and it is legal.

A real baseball pitched as in Fig. 11 will deflect by a smaller amount since it is much heavier than the polystyrene ball. However, if the side force coefficient $C_S = 0.2$ and if the ball is pitched at say 80 mph (35.8 ms^{-1}) then the ball will deflect sideways by 2 ft over the 60 ft distance from the pitcher to the batter. If the spin axis is tilted so that the

Magnus force adds to the total side force then the sideways deflection will be even larger. Experiments with real baseballs will be needed to quantify the magnitude of the side force more precisely, given that an artificial string seam on a polystyrene ball does not necessarily provide an accurate aerodynamic model of a real seam on a real baseball.

IX. CONCLUSION

Three relatively simple experiments have been described showing how the aerodynamics of a ball in flight can be conveniently studied or demonstrated using light polystyrene balls to minimize the effect of the gravitational force on the ball. It is easy to project a polystyrene ball at relatively high speed and it is safe to do so even in a classroom. Large, light balls can be projected at relatively low speed to examine the effects of the drag crisis and to observe how the Magnus force can sometimes be negative. The effect of a ball seam is also easy to study, simply by gluing a length of string around the ball, and it can be demonstrated that the side force arising from the seam changes direction at high ball speeds due to the onset of turbulence in the boundary layer on both sides of the ball. The effect of a baseball seam was also investigated and it was found that a side force can arise if the ball is pitched in such a way that one side of the ball remains smoother than the other.

X. ACKNOWLEDGEMENT

I would like to thank Professor Alan Nathan who provided me with the motivation to undertake these experiments by asking me why a baseball can sometimes break in the wrong direction and then telling me that my attempted explanations were crazy.

---

* Electronic address: cross@physics.usyd.edu.au

[1] L.J. Briggs, "Effect of spin and speed on the lateral deflection (curve) of a baseball; and the Magnus effect for smooth spheres," Am. J. Phys. **27**, 589–596 1959.

[2] R.G. Watts and E. Sawyer, "Aerodynamics of a knuckleball," Am. J. Phys. **43**, 960–963 (1975).

[3] C. Frohlich, "Aerodynamic drag crisis and its possible effect on the flight of baseballs," Am. J. Phys. **52**, 325–334 (1984).

[4] R.G. Watts and R. Ferrer, "The lateral force on a spinning sphere: Aerodynamics of a curveball," Am. J. Phys. **55**, 40–44 (1987).

[5] J.N. Libii, "Dimples and drag: Experimental demonstration of the aerodynamics of golf balls," Am. J. Phys. **75**, 764–767 (2007).

[6] H.M. Barkla and L.J. Auchterlonie, "The Magnus or Robins effect on rotating spheres," J. Fluid Mech. **47**, 437–447 (1971).

[7] R. Mehta, "Aerodynamics of sports balls," Ann. Rev. Fluid Mech. **17**, 151–189 (1985).

[8] L.W. Alaways and M. Hubbard, "Experimental determination of baseball spin and lift," J. Sports Sciences, **19**, 349–358 (2001).

[9] K. Takahashi and D. Thompson, "Measuring air resistance in a computerized laboratory," Am. J. Phys. **67**, 709–711 (1999).

[10] F.X. Hart and C.A. Little, "Student investigation of models for the drag force," Am. J. Phys. **44**, 872–878 (1976).

[11] M. Garg, P. Arun and F.M.S. Lima, "Accurate measurement of the position and velocity of a falling object," Am. J. Phys. **75**, 254–258 (2007).

[12] V. Pagonis and D. Guerra, "Effects of air resistance," Phys. Teach. **35**, 364-368 (1997).

[13] A. Nathan, "The effect of spin on the flight of a baseball," Am. J. Phys. **76**, 119–124 (2008).

[14] J.E. Goff and M.J. Carre, "Trajectory analysis of a soccer ball," Am. J. Phys. **77**, 1020–1027 (2009).

[15] J. R. Kensrud and L. V. Smith, "In situ drag measurements of sports balls," Procedia Engineering, **2**, 2437–2442 (2010).

[16] A.T. Sayers and A. Hill, "Aerodynamics of a cricket ball," J. Wind Engineering and Industrial Aerodynamics, **79**, 169–182 (1999).

[17] A.T. Sayers, "On the reverse swing of a cricket ball – modelling and measurements," J. Mech. Eng. Science, **215**, 45–55 (2001).

[18] R. Mehta, "An overview of cricket ball swing," Sports Engineering, **8**, 181–192 (2005).

[19] M.A Passmore, S. Tuplin, A. Spencer and R. Jones, "Experimental studies of the aerodynamics of spinning and stationary footballs," J. Mech. Eng. Science, **222**, 195–205 (2008).

[20] L.W. Alaways, "Aerodynamics of a curve–ball: An investigation of the effects of angular velocity on baseball trajectories," PhD Thesis, University of California Davis (1998). http://biosport.ucdavis.edu/lab-members/leroy-alaways

[21] M.P. Morrissey, "The aerodynamics of the knuckleball pitch: An experimental investigation into the effects that the seam and slow rotation have on a baseball," MSc Thesis, Marquette University, Wisconsin (2009). http://epublications.marquette.edu/theses_open/8/

[22] R.G. Watts and A.T. Bahill, *Keep your eye on the ball: the science and folklore of baseball* (Freeman N.Y. 1990).